01 Dec 1986

Calculation Of Electron Capture Cross Sections Of Collisions Of Be $^{2+}$ On H

A. E. Wetmore

H. R. Cole

Ronald E. Olson
Missouri University of Science and Technology, olson@mst.edu

Recommended Citation

A. E. Wetmore et al., "Calculation Of Electron Capture Cross Sections Of Collisions Of Be $^{2+}$ On H," *Journal of Physics B: Atomic and Molecular Physics*, vol. 19, no. 10, pp. 1515 - 1525, article no. 020, IOP Publishing, Dec 1986.
The definitive version is available at https://doi.org/10.1088/0022-3700/19/10/020

Calculation of electron capture cross sections of collisions of Be^{2+} on H

J. Phys. B: At. Mol. Phys. 19 (1986) 1515-1525. Printed in Great Britain

Calculation of electron capture cross sections for collisions of Be^{2+} and B^{3+} on H

A E Wetmore, H R Cole and R E Olson

Physics Department, University of Missouri-Rolla, Rolla, Missouri 65401, USA

Received 16 July 1985

Abstract. Using the perturbed stationary state method, including electron translation factors, we have calculated electron capture cross sections for the helium-like ions Be^{2+} and B^{3+} incident on ground-state atomic hydrogen. The molecular structure calculation employs pseudo-potentials to represent the inactive K-shell electrons on the incident ions. The calculated cross sections vary rapidly in the 10^7 cm s^{-1} velocity range ($E \sim 1$ keV amu^{-1}). Our calculations show preferential transfer to the $Be^+(2s)$ and the $B^{2+}(2p)$ product states. The calculations for $B^{3+}+H$ are in good agreement with experimental measurements of Crandall *et al.* In addition, the calculations indicate the importance of including rotational coupling to $^2\Pi$ states when determining state-to-state cross sections.

1. Introduction

We have studied the electron capture collision process,

$$X^{q+} + H(1s) \rightarrow X^{(q-1)+} + H^+ \tag{1}$$

where the multiply charged ion is either Be^{2+} or B^{3+}. These ions were chosen for this study because they are representative of the class of low atomic number systems which do not lend themselves to the application of scaling laws. One purpose of our calculations is to determine the product state (n, l) cross sections for charge transfer in the velocity range of 10^7-10^8 cm s^{-1} ($E \simeq 50$ eV amu^{-1}-5 keV amu^{-1}).

These partially stripped ions have a helium-like core of two electrons. The cross sections for these low charge state ions are dependent on the details of the molecular structure, especially the avoided crossings between molecular states. The perturbed stationary state (PSS) (Bates *et al* 1953) method was used to calculate the cross sections. The PSS method treats the collision in a molecular framework where the interatomic distance changes with time. At each time during the collision the transitions between all of the molecular states are computed. The transition probabilities are functions of the electronic potential energies and the non-adiabatic coupling matrix elements between the various molecular levels.

In our study we have treated the collision process as two ionic cores and a single valance electron. Gargaud *et al* (1981) and Kimura *et al* (1982) have shown that pseudo-potential methods can be used to compute accurate molecular wavefunctions and energies for similar systems. We have computed the wavefunctions and electronic potential energies at a large number of internuclear separations. These wavefunctions

0022-3700/86/101515+11$02.50

and energies were then used to calculate, at the same internuclear separations, the radial and rotational coupling matrix elements needed by the PSS method. The scattering equation was then integrated to obtain the probability of transitions to the various final states.

2. Pseudo-potential

We have used an l-dependent Gaussian pseudo-potential of the form

$$V(r, l) = a_l \exp(-b_l r^2) - \frac{\alpha_d}{2(r^2+d^2)^2} - \frac{\alpha_q}{2(r^2+d^2)^3} - \frac{q}{r} \tag{2}$$

to model the effect of the core electrons. This type of potential has been described by Bardsley (1974), and simulates the Pauli exclusion by the core electrons and also includes the core polarisation. The dipole and quadrupole polarisabilities, α_d and α_q, were taken from Dalgarno (1962). The cut-off parameter, d, serves to limit the range of the dipole and quadrupole polarisation forces, which originate with the core electrons, to the region outside of the core. The cut-off parameter used was the Hartree-Fock expectation value for the 1s (core) electrons (Froese Fischer 1977). q is the net ionic charge that will be seen by the valence electron at large r. The adjustable parameters a_l and b_l were calculated such that the ionisation energies of the two lowest states exactly match the values from spectroscopic measurements (Moore 1949). In all cases the next several ionisation energies were accurately predicted (within 1 meV). The pseudo-potential parameters used are given in table 1.

The quadrupole polarisabilities which we used are the static polarisabilities, not the dynamic polarisabilities which have been used in other molecular structure calculations (Pascale 1983, Peach 1982). Our choice is due to the lack of estimates of the dynamic polarisability for these systems which are accurate enough to improve upon the static polarisability (Dalgarno *et al* 1968). As a test of the sensitivity of the molecular structure calculations to the value of the quadrupole polarisability we calculated the pseudo-potential parameters totally neglecting the quadrupole polarisability. Using these values in the molecular structure calculation, the electronic energies differed by less than 0.001 Hartree from the values obtained using the pseudo-potential parameters in table 1. These small differences, which are comparable with what would be obtained

Table 1. Pseudo-potential parameters (in atomic units).

	Be^{2+}	B^{3+}
a_0	13.964 744	24.426 318
a_1	−0.420 099 82	−1.523 8484
a_2	−0.000 386 188 39	−0.769 744 79
b_0	2.683 0881	4.528 4976
b_1	1.630 5872	4.969 0687
b_2	0.117 082 36	5.000 0000
q	2.0	3.0
d	0.385	0.326
α_d	0.051 20	0.0194
α_q	0.015 32	0.003 37

using a dynamic polarisability, are not expected to alter the results of the scattering calculation significantly.

3. Wavefunctions

An optimised Slater-type orbital (STO) basis set and standard variational methods were used to calculate the Born-Oppenheimer molecular wavefunctions, ϕ_i^{BO}, and electronic potential energies, E_i, as a function of the internuclear separation. The H basis set is exact through the $n = 2$ level and included a tight 2p function, $\xi = 1.0$, to improve the dipole polarisability of H. For the two ions, Be^{2+} and B^{3+}, the 2s functions were obtained from Clementi and Roetti (1974). The 2p functions were obtained by optimising the wavefunctions to obtain the lowest energy for the 2p states. The $n = 3$ and $n = 4$ terms were simply determined using quantum defect theory. The STO basis sets used in the molecular structure calculations are shown in table 2. The molecular structure calculations reproduced the asymptotic energy levels to within 0.03 eV, except for the $B^{2+}(2s)$ level which differed from the spectroscopic level by 0.06 eV.

Table 2. Slater-type orbital basis sets.

H		Be^{2+}		B^{3+}	
1s	2.000	2s	6.489	2s	7.936
	1.000		2.628		3.486
	0.500		1.184		1.722
2s	0.500		0.627		1.071
2p	1.000	2p	2.080	2p	3.699
	0.500		1.033		1.569
		3s	0.713		1.015
		3p	0.623	3s	1.071
		3d	0.670	3p	1.015
				3d	1.001
				4s	0.789
				4p	0.758

The electronic wavefunctions used in the scattering equation were described using electron translation factors (ETF), retaining all terms to first order in the velocity. The form used was

$$\phi_i(r, t) = \sum_i a_i(t)\phi_i^{BO}(\boldsymbol{r}, \boldsymbol{R})F_i(\boldsymbol{r}, \boldsymbol{R}) \tag{3}$$

where $F_i(\boldsymbol{r}, \boldsymbol{R})$ is the electron translation factor (ETF) as described by Kimura and Thorson (1981). The Born-Oppenheimer molecular wavefunctions,

$$\phi^{BO}(\boldsymbol{r}, \boldsymbol{R}) = \sum_j b_j(R)\,\mathrm{STO}(j) \tag{4}$$

were used in (3) to calculate the electronic wavefunctions, ϕ_i, which include the ETF.

4. Scattering equations

The time evolution of the system during the collision is governed by the scattering

equation,

$$i\hbar\dot{a}_k(t) = \sum_{n\neq k} \boldsymbol{V}\cdot(\boldsymbol{P}+\boldsymbol{A})_{kn}a_n(t)\exp\left(\frac{-i}{\hbar}\int^t (E_n - E_k)\,dt\right) \tag{5}$$

where

$$\boldsymbol{P}_{kn} = \langle k|-i\hbar\boldsymbol{\nabla}_R|n\rangle \tag{6}$$

and

$$\boldsymbol{A}_{kn} = (im/\hbar)(E_k - E_n)\langle k|\tfrac{1}{2}f_n(\boldsymbol{r},\boldsymbol{R})\boldsymbol{r}|n\rangle \tag{7}$$

are the coupling matrix elements. The coupling matrix elements can be separated into radial and rotational terms which describe the $^2\Sigma$-$^2\Sigma$ and $^2\Sigma$-$^2\Pi$ transitions.

The unmodified wavefunctions were used to calculate the radial,

$$(\boldsymbol{P}+\boldsymbol{A})_{kn} = \frac{-i\hbar}{(E_n - E_k)}\langle k|\,dH_{el}/dR|n\rangle + \frac{im}{\hbar}(E_k - E_n)\langle k|zf_n(\boldsymbol{r},\boldsymbol{R})|n\rangle \tag{8}$$

and rotational,

$$(\boldsymbol{P}+\boldsymbol{A})_{kn} = \frac{-1}{R}\langle k|\hat{L}_y|n\rangle + \frac{im}{\hbar}(E_k - E_n)\langle k|xf_n(\boldsymbol{r},\boldsymbol{R})|n\rangle \tag{9}$$

coupling matrix elements as functions of the internuclear separation. In equations (8) and (9) the second term is from the electron translation factors.

The cross sections were calculated by integrating (5) along straight-line trajectories. Since the impact parameter and classical turning point, R_0, are related through

$$b = R_0(1 - V(R_0)/E)^{1/2} \tag{10}$$

only very small impact parameter collisions will be changed in the keV energy range by the use of curvilinear trajectories. The integration was carried out for a range of impact parameters, b, to obtain the probability, $P_k(b)$, of a transition to the kth state. Integrating $P_k(b)$ from 0 to b_{max} yields the kth cross section. The total cross sections were then obtained by summing the partial cross sections.

5. $Be^{2+} + H \rightarrow Be^{+} + H^{+}$

Figure 1 shows the electronic potential energy curves for BeH^{2+}. These were calculated using the Slater-type orbital basis set given in table 2. The most important feature is the avoided crossing between the $Be^{+}(2s)$ and H(1s) states which occurs at an internuclear separation of 6.75 au. This avoided crossing is shown in greater detail in figure 2. The avoided crossing leads to most of the depopulation of the H(1s) incident channel.

The trajectories of small impact parameter collisions allow rotational coupling at small internuclear separations to populate the $Be^{+}(2p)$ $^2\Pi$ exit channel. At low energies this is an important mechanism for excitation to the $Be^{+}(2p)$ state and, although the total cross section is small, most of the $Be^{+}(2p)$ cross section is in the $Be^{+}(2p)$ $^2\Pi$ state. This is also the class of collisions that will have the largest errors from using the straight-line trajectory approximation.

The coupling matrix elements for the dominant processes are shown in figures 3 and 4. In figure 3 the radial $(\partial/\partial R)$ coupling matrix elements between the $Be^{+}(2s)$ and H(1s) channels which peak near the internuclear separation of 7 au and the coupling

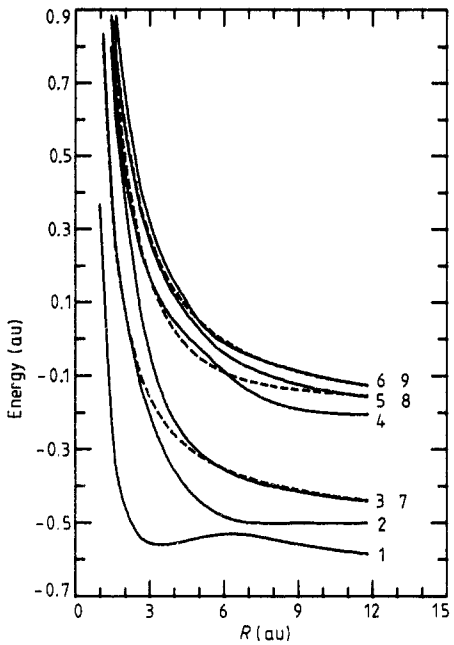

Figure 1. Electronic potential energies for BeH^{2+}. Full curves are $^2\Sigma$ states, broken curves are $^2\Pi$ states. 1, $Be^+(2s)+H^+$; 2, $Be^{2+}+H(1s)$; 3, $Be^+(2p)+H^+$; 4, $Be^+(3s)+H^+$; 5, $Be^+(3p)+H^+$; 6, $Be^+(3d)+H^+$; 7, $Be^+(2p)+H^+$, 8, $Be^+(3p)+H^+$; 9, $Be^+(3d)+H^+$.

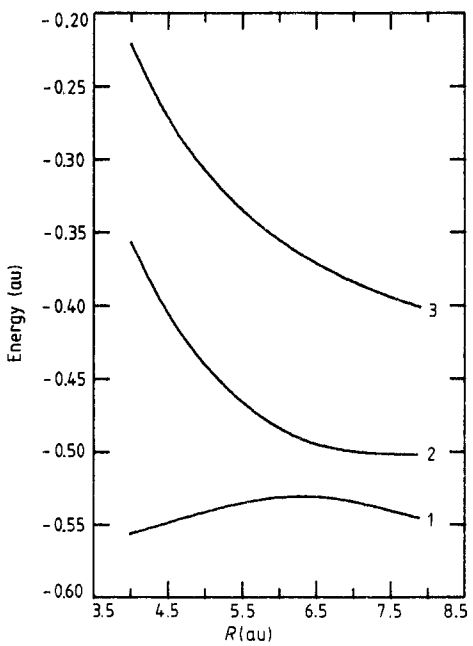

Figure 2. The avoided crossing in the BeH^{2+} potential energy curves at 6.75 au internuclear separation. The identification of the states is the same as in figure 1.

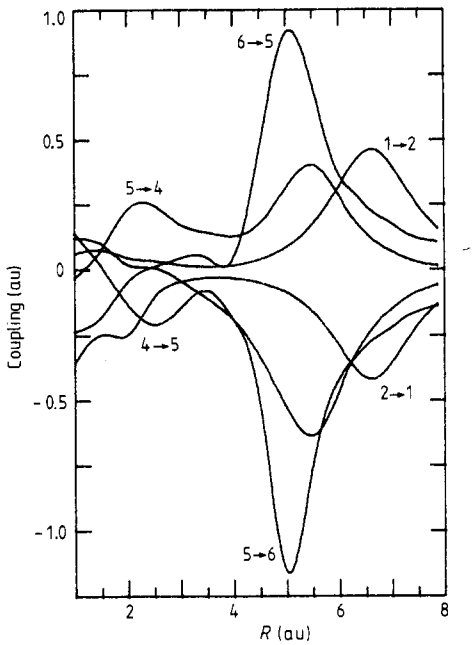

Figure 3. The important radial coupling matrix elements for BeH^{2+}.

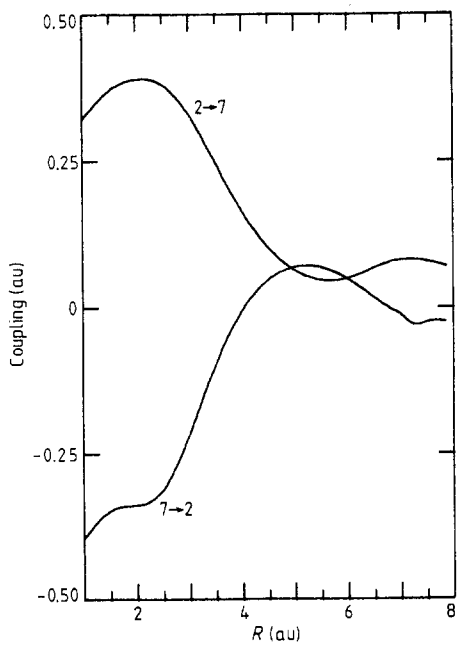

Figure 4. The important rotational coupling matrix elements for BeH^{2+}.

between the $Be^+(n=3)$ channels with peaks near the internuclear separation of 5 au are shown. Figure 4 shows the rotational coupling between the H(1s) and $Be^+(2p)\ ^2\Pi$ states. Because the coupling is limited to small internuclear separations only collisions at small impact parameters will be affected by this process.

At low energies the $2p\ ^2\Pi$ cross section accounts for approximately 15% of the total, with the remaining 85% going predominantly into the $Be^+(2s)\ ^2\Sigma$ state. As the energy increases the number of states which have significant population increases, until at the highest energies the $Be^+(2s)\ ^2\Sigma$ state accounts for only about 35% of the total cross section. Figure 5 shows the total, 2s and 2p charge transfer cross sections. In addition the cross sections calculated in 1954 by Bates and Moiseiwitsch using the Landau-Zener approximation, and the two-state calculation of Bates *et al* (1964) are shown. These two calculations were for the $B^{2+}+H \rightarrow Be^+(2s)+H^+$ reaction. The peak in our cross section is 25×10^{-16} cm^2, approximately the same magnitude as the two-state calculation of Bates *et al* (1964). Our peak position differs considerably from the earlier work.

6. $B^{3+}+H \rightarrow B^{2+}+H^+$

The electronic potential energy curves for the BH^{3+} system are shown in figure 6. These were calculated using the Slater-type orbital basis set given in table 2. Unlike the case with the $Be^{2+}+H$ system the avoided crossings between the H(1s) initial

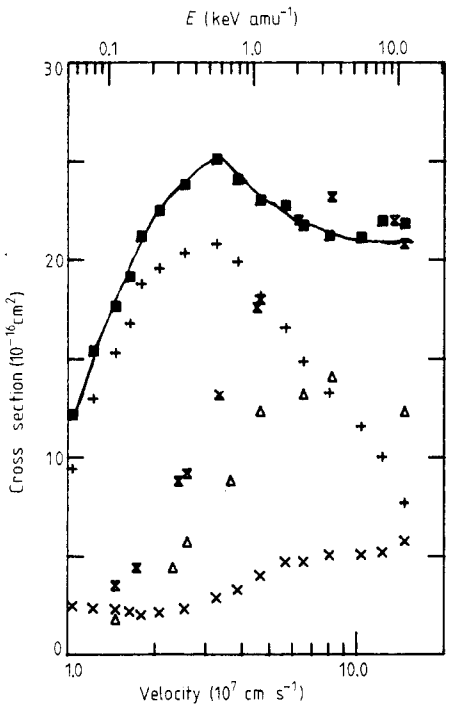

Figure 5. The calculated cross section for: ■, $Be^{2+}+H \rightarrow Be^+ + H^+$; +, $Be^{2+}+H \rightarrow Be^+(2s)+H$; ×, $Be^{2+}+H \rightarrow Be^+(2p)+H^+$. Also shown are the results of the Landau-Zener calculation of Bates and Moiseiwitsch (1954) (△) and the two-state calculation of Bates *et al* (1964) (⧖) for the $Be^{2+}+H \rightarrow Be^+(2s)+H^+$ reaction.

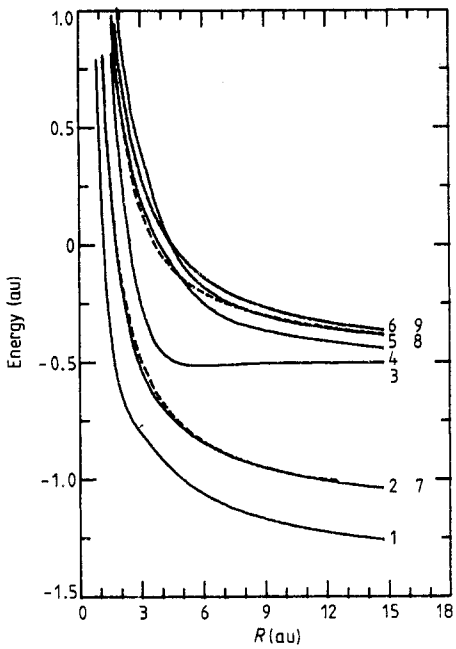

Figure 6. Electronic potential energies for BH^{3+}. Full curves are $^2\Sigma$ states, broken curves are $^2\Pi$ states. 1, $B^{2+}(2s)+H^+$; 2, $B^{2+}(2p)+H^+$; 3, $B^{3+}+H(1s)$; 4, $B^{2+}(3s)+H^+$; 5, $B^{2+}(3p)+H^+$; 6, $B^{2+}(3d)+H^+$; 7, $B^{2+}(2p)+H^+$; 8, $B^{2+}(3p)+H^+$; 9, $B^{2+}(3d)+H^+$.

channel and the $B^{2+}(n=2)$ channels are found at small (4.0 au) internuclear separations. Because only small impact parameter collisions will pass through this region, the cross section to $n=2$ states will be smaller than in the BeH^{2+} case.

Several of the radial matrix elements for BH^{3+} are shown in figure 7. The coupling between the incident H(1s) state and the $B^{2+}(2p)$ state occurs near an internuclear separation 4 au. The radial coupling at the avoided crossing between the $B^{2+}(2p)$ and H(1s) states is weaker than in the $Be^+(2s)$-H(1s) case. The strong coupling at 1.25 au is between the H(1s) and $B^{2+}(3s)$ states. The coupling between the $B^{2+}(3p)$ and $B^{2+}(3d)$ states takes place at an internuclear separation of 4.4 au.

Figure 8 shows the most important rotational coupling matrix elements. There is strong rotational coupling between the H(1s) and the $B^{2+}(2p)$ $^2\Pi$ state. In addition, the rotational coupling from the H(1s) to $B^{2+}(3p)$ $^2\Pi$ state is shown as well as coupling within the final states of the $B^{2+}(n=3)$ manifold.

Figure 9 displays the total calculated cross section. At the lowest energies, $E \leqslant$ 220 eV, 90% of the charge transfer is to the $B^{2+}(n=3)$ states and 10% to the $B^{2+}(2p)$ state. At 550 eV the $B^{2+}(2p)$ cross section accounts for 55% of the total with 45% going into the $n=3$ manifold. From 1000 to 5000 eV the cross section remains partitioned between the 2p state, with 70% of the cross section, and the $n=3$ states, with 30% of the cross section. At 7000 eV and above the 2s state begins to increase to around 10% of the total cross section at the expense of the 2p state. The $n=3$ manifold continues to contribute about 30% of the cross section. Our calculations of the total cross section agree quite well with both the experimental results of Crandall *et al* (1979) and the earlier eight-state close coupling calculation of Olson *et al* (1978) which used *ab initio* potential energy curves but did not include electron translation factors.

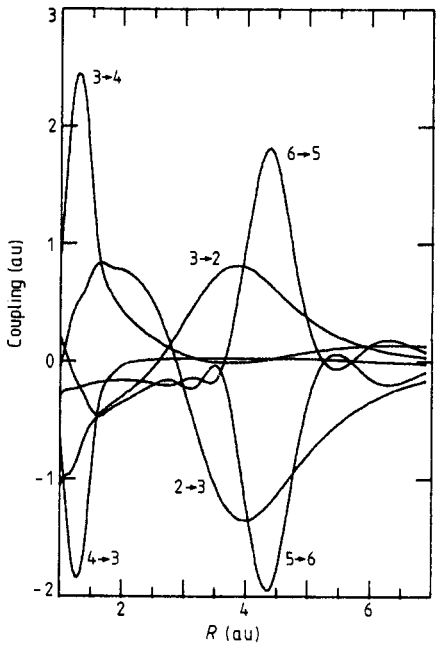

Figure 7. Important radial coupling matrix elements for BH^{3+}. The $\langle 2|3\rangle$ and $\langle 3|2\rangle$ matrix elements are shown at five times actual size.

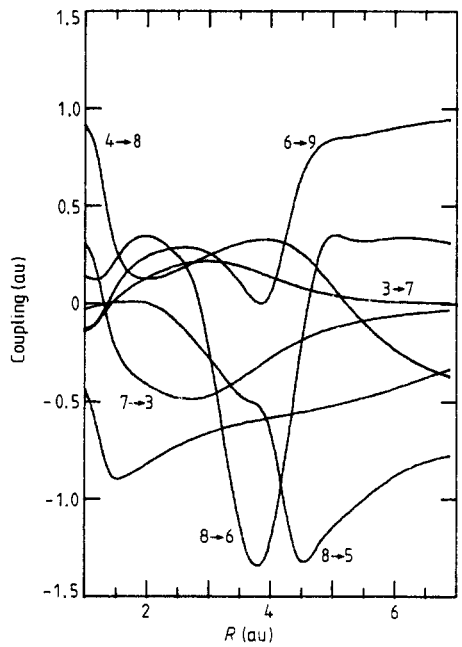

Figure 8. Rotational coupling matrix elements for BH^{3+}.

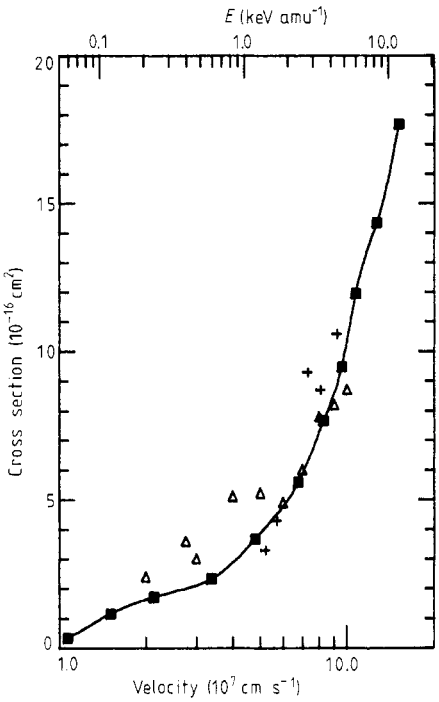

Figure 9. The total cross section for $B^{3+} + H \rightarrow B^{2+} + H^+$ change transfer (■). Also shown are the experimental data of Crandall *et al* (1979) (+) and the calculation of Olson *et al* (1978) (△).

7. Conclusions

Standard pseudo-potential and molecular structure techniques were used to calculate the Born-Oppenheimer eigenfunctions and energy levels for the $Be^{2+} + H$ and $B^{3+} + H$ systems. These molecular representations were utilised in a calculation of the coupling coefficients for the perturbed stationary state method. The cross sections obtained from the PSS method show that state to state cross sections are highly dependent on both the collision energy and the collision partners. Also, our results show that including rotational coupling to $^2\Pi$ states is extremely important. Good agreement with experiment is realised for the $(BH)^{3+}$ system.

Acknowledgments

This work was supported by the Office of Fusion Energy of the United States Department of Energy.

References

Bardsley J N 1974 *Case Studies At. Phys.* **4** 299-368
Bates D R, Johnston H C and Stewart I 1964 *Proc. Phys. Soc.* **84** 517-25
Bates D R, Massey H S W and Stewart A L 1953 *Proc. Phys. Soc.* A **216** 437-58

Bates D R and Moiseiwitsch B L 1954 *Proc. Phys. Soc.* **67** 805-12
Clementi E and Roetti C 1974 *At. Data Nucl. Data Tables* **14** 177-478
Crandall D H, Phaneuf R A and Meyer F W 1979 *Phys. Rev.* A **19** 504-14
Dalgarno A 1962 *Adv. Phys.* **2** 281-315
Dalgarno A, Drake G W F and Victor G A 1968 *Phys. Rev.* **176** 194-7
Froese Fischer C 1977 *The Hartree-Fock Method for Atoms* (New York: Wiley-Interscience)
Gargaud M, Hanssen J, McCarrol R and Valiron P 1981 *J. Phys. B: At. Mol. Phys.* **14** 2259-76
Kimura M, Olson R E and Pascale J 1982 *Phys. Rev.* A **26** 3113-24
Kimura M and Thorson W R 1981 *Phys. Rev.* A **24** 1780-92
Moore C E 1949 *Atomic Energy Levels* NBS Circular No 467, vol 1 (Washington, DC: US Govt Printing Office) pp 14, 19
Olson R E, Shipsey E J and Browne J C 1978 *J. Phys. B: At. Mol. Phys.* **11** 699-708
Pascale J 1983 *Phys. Rev.* A **28** 623-44
Peach G 1982 *Comment. At. Mol. Phys.* **11** 101-18